General Disclaimer

One or more of the Following Statements may affect this Document

- This document has been reproduced from the best copy furnished by the organizational source. It is being released in the interest of making available as much information as possible.

- This document may contain data, which exceeds the sheet parameters. It was furnished in this condition by the organizational source and is the best copy available.

- This document may contain tone-on-tone or color graphs, charts and/or pictures, which have been reproduced in black and white.

- This document is paginated as submitted by the original source.

- Portions of this document are not fully legible due to the historical nature of some of the material. However, it is the best reproduction available from the original submission.

NASA

Technical Memorandum **80326**

The Shape and Location of the Sector Boundary Surface in the Inner Solar System

U. Villante, R. Bruno, F. Mariani, L. F. Burlaga and N. F. Ness

JULY 1979

National Aeronautics and Space Administration

Goddard Space Flight Center
Greenbelt, Maryland 20771

THE SHAPE AND LOCATION OF THE SECTOR BOUNDARY SURFACE IN THE INNER SOLAR SYSTEM

U. Villante (*)
R. Bruno
Istituto Fisica, Universita, L'Aquila

F. Mariani(*)
Istituto Fisica, Universita, Roma

L.F. Burlaga
N.F. Ness
NASA/Goddard Space Flight Center
Greenbelt, MD 20771

(*) Also at Laboratorio Plasma nello Spazio, CNR, Frascati

5370 Solar wind magnetic fields

THE SHAPE AND LOCATION OF THE SECTOR BOUNDARY SURFACE IN THE INNER SOLAR SYSTEM

U. Villante (Istituto Fisica, Universita, L'Aquila) R. Bruno, F. Mariani, L. F. Burlaga and N. F. Ness.

Simultaneous observations by Helios-1 and Helios-2 over four solar rotations, between Jan. 20 and May 23, 1976, were used to determine the latitudinal dependence of the polarity of the interplanetary magnetic field within $\pm$ 7.23° of the solar equator and within 1 AU. The longitudinal and latitudinal positions of the sector boundary crossing are consistent with a warped sector boundary which extended from the sun to 1 AU and was inclined $\approx$ 10° with respect to the heliographic equator. This is consistent with simultaneous Pioneer 11 observations, which showed unipolar fields at latitude $\approx$ 16° at heliocentric distances greater than 3.5 AU. Two sectors were observed at southern latitudes; however, four sectors were observed at northern latitudes on two rotations, indicating a distortion from planarity of the sectory boundary surface.

(sector boundaries, solar wind, magnetic fields).

INTRODUCTION

Wilcox and Ness, (1965), first identified the by now well known sector structure of the interplanetary magnetic field (IMF, hereafter). Schulz (1973) and more recently Levy (1976) and Alfven (1977) proposed that the sector pattern is due to a near-equatorial, warped (non-planar) surface or current layer (similar to the skirt of a spinning ballerina) separating two solar hemispheres of opposite field polarities. In this picture the observed field polarity is determined by the position of the observing spacecraft relative to the current layer and not only the latitude relative to the equatorial plane. In this model,the IMF is considered to be a simple extension of a general dipole-like field of the Sun; hence inward (outward) field lines would be expected at high negative (positive) heliographic latitudes during this part of the solar cycle.

The Schulz-Levy-Alfven model is grossly consistent with the latitudinal dependence of the IMF polarity observed by Rosenberg and Coleman,1969 and Rosenberg, 1975), and it is strongly supported by the experimental observations performed by Pioneer 11 after its encounter with Jupiter. Smith et al., (1978) and Smith (1979), considering quick look data samples of the IMF, showed an almost total absence of inward field lines at 16^{o} above the solar equatorial plane.

In this paper we compare the IMF polarities measured simultaneously by the University of Rome/GSFC magnetometer on the solar probes Helios 1 and 2 in the period Jan. 20 through May 23, 1976, which roughly corresponds to the primary mission of Helios 2. Our high resolution and nearly complete data coverage provide a unique opportunity to study the near-Sun region at the time when Pioneer 11 was monitoring the interplanetary medium with lower resolution and at larger heliocentric distances and latitudes. The Helios-1 and -2 trajectories in the period of interest were confined between 0.28 and 1 AU, with a latitudinal excursion of $\pm 7.23^{o}$ from the solar equatorial plane. Observations made simultaneously at different

heliographic latitudes provide information about the orientation and shape of the sector boundary surface separating regions of opposite field polarities.

The IMF observations made by Helios-1 and -2 and their relationship to the stream structure and the coronal holes pattern have been already discussed in papers by Mariani et al., (1978a, 1978b); Burlaga et al., (1978b); and Villante et al., (1978). These papers also give details about spacecraft trajectories, instrumentation and data reduction.

A Comparison of the IMF Polarities Observed by Helios-1 and -2.

The IMF pattern observed by Helios-1 and -2 in the period of interest is shown in Figure 1. Twelve hour averages of the magnetic field parameters, computed when at least 3 hours of data were available, are plotted versus the solar longitude of the spacecraft at the time of the observations. Four solar rotations were observed. The Helios-1 and -2 magnetic field polarity data may be compared without correction for their radial separation and the varying solar wind speed if conditions were stationary over time intervals of several days. In this respect, it is significant rthat Schwenn et al. (1977), reported clear evidence for stationarity of the stream profiles observed by the two spacecraft during the primary mission phase of Helios 2. The Helios 2 magnetic field observations (which are less affected by the data gaps than Helios 1) are consistent with a steardy-state character of the source regions located in the solar corona, since the gross shape of the IMF was essentially the same during the first, second and third solar rotations. In that period of time, Helios 2 travelled between the earth's orbit and 0.29 AU. Thus, the invariance of the magnetic field pattern also implies that the general shape of the unipolar regions of the IMF was not dependent on heliocentric distance within 1 AU. This result is confirmed by a comparison of simultaneous Helios-1 and Helios-2 observations.

The boundary crossings between regions of opposite Φ-polarities appear very sharp in Figure 1, where 12-hour averages of the field elements are

shown. Inspection of data with higher time resolution, however, shows that single crossings occurred over time intervals between a few minutes and several hours. There is no clear relationship between the boundary thickness and the heliocentric distance. A thorough discussion of the internal structure of the boundary layers is deferred to another paper.

Figures 1a and 1b show very good agreement between the observed Φ-polarities during the first and second solar rotations, when both spacecraft were located below the solar equatorial plane (The difference of heliocentric distances varied between $\sim$ .05 and $\sim$ .25 AU in that period of time). There is no such agreement during the third solar rotation (Figure 1c), when both spacecraft rapidly moved (at different times) from negative (southern) to positive (northern) heliographic latitudes. A large region of inward field lines was observed below the solar equatorial plane by Helios 2, whereas two smaller regions of inward field lines separated by a region of outward field lines were observed above the solar equatorial plane by Helios 1 at the corresponding longitudes.

The longitudinal and latitudinal extent of the source regions can be estimated by projecting the ϕ-polarities observed in the interplanetary medium onto the solar corona. We made this projection using the hourly average values of both the field elements and the solar wind speed (Rosenbauer, private communication); we used an angular velocity Ω_s (α) corresponding to the heliographic latitude of the observing spacecraft, and we assumed that the solar wind speed did not vary with distance. Variations of the field polarities which lasted less than 6 hours have been disregarded in our analysis. The experimental results are shown in Figure 2.

Observations made on the third solar rotation (Figure 2) dramatically show the latitudinal dependence of the IMF polarities. Below the equator, a 2-sector pattern was observed, whereas above the equator a 4-sector pattern was observed. The 2-sector pattern at negative latitudes ($\geq -7.3^{\circ}$) persisted through rotations 1, 2, and 3 and for part of rotation 4. The 4-sector pattern at positive latitudes ($< 7.3^{\circ}$) persisted through rotations 3 and 4. Thus, the sector pattern was relatively stable, and the observations clearly indicate strong latitudinal variations (rather than time variations) on rotation 3.

On the Shape of the Sector Boundary Surface

The macroscale features of the surface separating regions of opposite field polarities can be estimated considering a) the number of unipolar regions (as projected onto the solar corona) per solar rotation, b) their longitudinal extension, and c) the locations of the boundary crossings. As suggested by Smith and Wolfe, (1978), the observation of only two regions of dominant polarity per solar rotation may be interpreted in terms of a planar sector boundary surface which is tilted at an angle β with respect to the solar equator and rotates with the sun. The intersection of the sector boundary plane with a sun-centered sphere is a circle. A line from the center of the sphere to the circle makes an angle α_B with the solar equatorial plane, and α_B varies with longitude, Λ, as $\alpha_B = \beta \sin \Lambda$. In this model, the percentage of fields of a given polarity observed by a spacecraft at latitude $\alpha_{S/C}$ is a function of $\alpha_{S/C}$ and β. In particular, if the spacecraft intersects the sector boundary plane at longitudes Λ_1 and Λ_2, then the fraction of field lines with the polarity observed in that interval should be $f = (\Lambda_2 - \Lambda_1)/360 = (180 - 2\Lambda_1)/360 = 0.5 - (1/180) \sin^{-1} (\alpha_{S/C}/\beta)$. When the spacecraft is at the equator, $f = 0.5$, and when its latitude is $> \beta$, the spacecraft would see only one polarity.

Two sectors were observed on rotations 1 and 2 when Helios-1 and -2 were at heliographic latitudes between $\alpha_{S/C} = -5.0^\circ$ and $\alpha_{S/C} = -7.23^\circ$. During the whole solar rotation identified by the arrows in Figure 2, the latitude of Helios-2 was nearly constant at $\simeq -7^\circ$ and the data coverage was almost complete. The fraction of longitudes in which positive fields were observed was $f \simeq 0.3$. Solving the equation in the preceding paragraph for β, with $f = 0.3$ and $\alpha_{S/C} = -7^\circ$, gives $\beta \simeq 12^\circ$. For $\alpha = -5^\circ$ and $f = 0.3$, $\beta = 8.5^\circ$. These numbers are consistent with the results of Pioneer 11 during the same period, which observed a single polarity at latitude $\simeq 16^\circ$.

Since the sector pattern was nearly stationary during rotations 1-4, it is meaningful to plot the positions of all the observed sector boundary crossings on a single latitude (α) versus longitude (Λ) plot and to compare them with the plane sector boundary model. Figure 3 shows the projected boundary crossings (α_s, Λ_s), taken from Figure 2. The sine curve in that

figure represents the intersection of a plane sector boundary (inclined at $\beta = 10^{\circ}$ with respect to the solar equator) with the surface of the sun. The observed current sheet crossings are within a few degrees of those predicted by the model.

The scatter of points in Figure 3 about the sine curve is real, and it suggests the existence of small local distortions of the sector boundary. In particular, a distortion must be assumed to account for the 4-sector pattern observed at northern latitudes; a relatively small distortion would suffice. Figure 4a shows a 3-dimensional view of the hypothetical undistorted boundary surface with respect to the sun. Figure 4b is one possible configuration for the inferred distorted boundary surface (a relatively extreme case), which would give a 4-sector pattern for a spacecraft at certain positive latitudes, a 2-sector pattern at certain negative latitudes, and scatter about the model curve at all latitudes.

Summary and Discussion

The experimental observations performed by Helios 1 and Helios 2 spacecraft allow a significant improvement in our knowledge of the latitudinal dependence of the IMF polarity. Both longitudinal and latitudinal boundaries of the unipolar regions of the IMF can be clearly identified in the experimental data. The availability of the simultaneous plasma data allowed us to project the field polarities observed in the interplanetary medium onto the solar corona. This is important because the longitudinal widths of the interplanetary structures do not necessarily correspond to the longitudinal widths of the source regions located in the solar corona, due to variations of the solar wind speed. This effect increases with heliocentric distance.

The principal conclusions of our investigation are as follows:

1. Helios observations confirm (see also Villante et al., 1978) that the latitudinal dependences of the IMF polarity extend to the inner solar system, and they show that the longitudinal widths of the unipolar regions were independent of the heliocentric distance.

2. The percentage of field lines of a given polarity, and the latitudes and longitudes of the projected sector boundary crossings, are consistent with a sector boundary surface that was nearly planar and inclined about 10° with respect to the heliographic equator. This is consistent with simultaneous Pioneer 11 observations made beyond 5 AU, which showed unipolar fields at a latitude of 16°.

3. The projection of the IMF polarities to the sun shows that on two rotations two regions of dominant polarity were observed several degrees below the solar equatorial plane, whereas four regions of dominant polarity were observed several degrees above the plane at the same time. This can be explained by postulating a distortion in the sector boundary surface at positive latitudes.

We caution that a plane sector boundary surface is just one of the

possible models which can be invoked to interpret the IMF polarities. For example, in previous papers (Villante et al., 1978; Burlaga et al., 1978b), we reported detailed evidence for a clear correspondence between the IMF polarities and the corresponding coronal holes pattern during the primary mission of Helios 1, namely Dec. 74 through April 75. Such a correspondence has also been discussed by other authors (see the review by Hundhausen, 1977). Burlaga et al., (1978a) have discussed a possible relation between the shape of the sector boundary surface and the positions of coronal holes. In this sense the occurrence of four or more regions of dominant polarity per solar rotation at positive latitudes might be better interpreted in terms of the coronal hole configuration. In any case, caution should be adopted when the average inclination of the sector boundary with respect to the solar equator is estimated by considering the percentages of field lines of an assigned polarity, since these percentages might be affected by the divergence of fields from isolated structures as they are extended from the inner corona to the interplanetary medium.

References

Alfven, H., Electric current in cosmic plasmas, Rev. Geophys. Space Phys., 15, 271, 1977.

Burlaga, L.F., K.W. Behannon, S.F. Hansen, G.W. Pneuman, and W.C. Feldman, Sources of magnetic fields in recurrent interplanetary streams, J. Geophys. Res., 83, 4177, 1978a.

Burlaga L.F., N.F. Ness, F. Mariani, B. Bavassano, U. Villante, H. Rosenbauer, R, Schwenn, and J. Harvey, Magnetic fields and flows between 1 and 0.3 AU during the primary mission of Helios 1, J. Geophys. Res., 83, 5167, 1978b.

Hundhausen, A.J., An interplanetary view of coronal holes, in Coronal Holes and High Speed Solar Wind Streams, edited by J.B. Zirker, p. 298, Colorado Universities Press, Boulder, 1977.

Levy, E. H., The interplanetary magnetic field structure, Nature, 261, 394, 1976.

Mariani, F., N.F. Ness, L. F. Burlaga, B. Bavassano, and U. Villante, The large-scale structure of the interplanetary magnetic field between 1 and 0.3 AU during the primary mission of Helios 1, J. Geophys., Res., 83, 5167, 1978a.

Mariani F., U. Villante, R. Bavassano, N.F. Ness, and L.F. Burlaga, An extended investigation of Helios 1 and 2 observations: the interplanetary magnetic field Between 0.3 and 1 AU, Solar Phys., (in press), 1978b.

Rosenberg, R. L., Latitude dependence of IMF dominant polarity, J. Geophys. Res., 10, 1339, 1975.

Rosenberg, R.L., and P.J. Coleman, Heliographic latitude dependence of the dominant polarity of the interplanetary magnetic field, J. Geophys. Res., 74., 5611, 1969.

Schulz M., Interplanetary sector structure and the heliomagnetic equator, J. Geophys. Res., 24, 371, 1973.

Schwenn, R., H. Rosenbauer, and K. H. Muhlhauser, The solar wind during STIP II interval: Stream structures, boundaries, shocks and other features as poserved by the plasma instruments on Helios 1 and Helios 2, COSPAR Symposium B, Tel Aviv, Israel, 1977.

Smith, E.J., and J.H. Wolfe, Fields and particles in the outer solar system, Space Sci. Rev., 23, 217, 1979.

Smith, E.J., Solar wind magnetic field observations, to appear in Solar Wind IV, 1979.

Villante U., F. Mariani, L. F. Burlaga, and N.F. Ness, IMF structures between 0.3 and 1 AU. A comparison of two-spacecraft observations, Nuovo Cimento, 1, 261, 1978.

Wilcox, J. M. and N.F. Ness, Quasi-stationary corotating structure in the interplanetary medium, J. Geophys. Res., 70, 5793, 1965.

Acknowledgements

Authors are grateful to Drs. H. Rosenbauer and R. Schwenn (Max Planck Institute, Lindau, West Germany) for the hourly average data of the solar wind parameters, as distributed to the Helios experimenters. We also thank Dr. B. Bavassano (Laboratorio Plasma nello Spazio, CNR, Frascati) for helpful discussions.

Figure Captions

Figure 1 12-hr averages of the field elements organized by solar rotation (α_S is the heliographic latitude of the observing spacecraft). Here B is the field magnitude, θ is the inclination of the magnetic field with respect to the ecliptic plane (positive for a northward direction) and ϕ, which defines the polarity of the interplanetary magnetic field, is the angle of the ecliptic plane component of the magnetic field with the radial direction ($\phi = 0^\circ$ corresponds to a sunward orientation).

Figure 2 The interplanetary magnetic field polarity, projected onto the solar corona. Here α_S is the heliographic latitude of the observing spacecraft while Λ_S is the solar (Carrington) longitude corresponding to a back projection of the fields made using the measured solar wind velocity.

Figure 3 The solar projected latitudes and longitudes of the sector boundary crossings observed by Helios-1 and -2. If the sector boundary were a plane inclined 10° with respect to the solar equator and rotating with the sun, then the observed crossings would lie on the sine curve shown here.

Figure 4a The idealized shape of a planar current sheet which is tilted at 10° with respect to the solar equator as it is observed in the interplanetary medium over a solar rotation.

Figure 4b The shape of the current sheet as extrapolated from the location of the boundary crossings; the orientation of the local normals to the current sheet; and the longitudinal extension of the unipolar regions of the interplanetary magnetic field. Solid lines correspond to the region of direct knowledge of the current sheet by Helios observations.

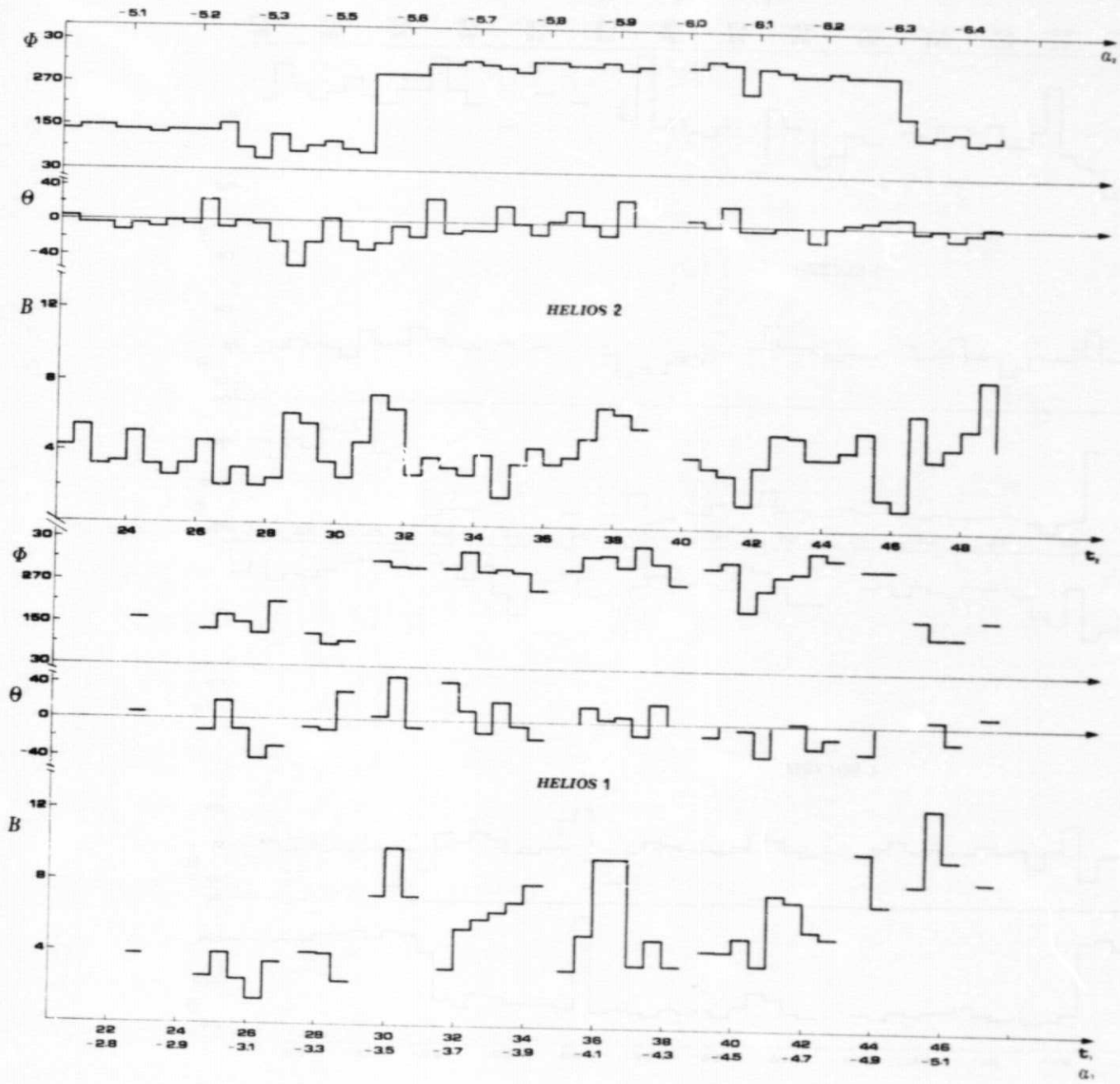

Figure 1a

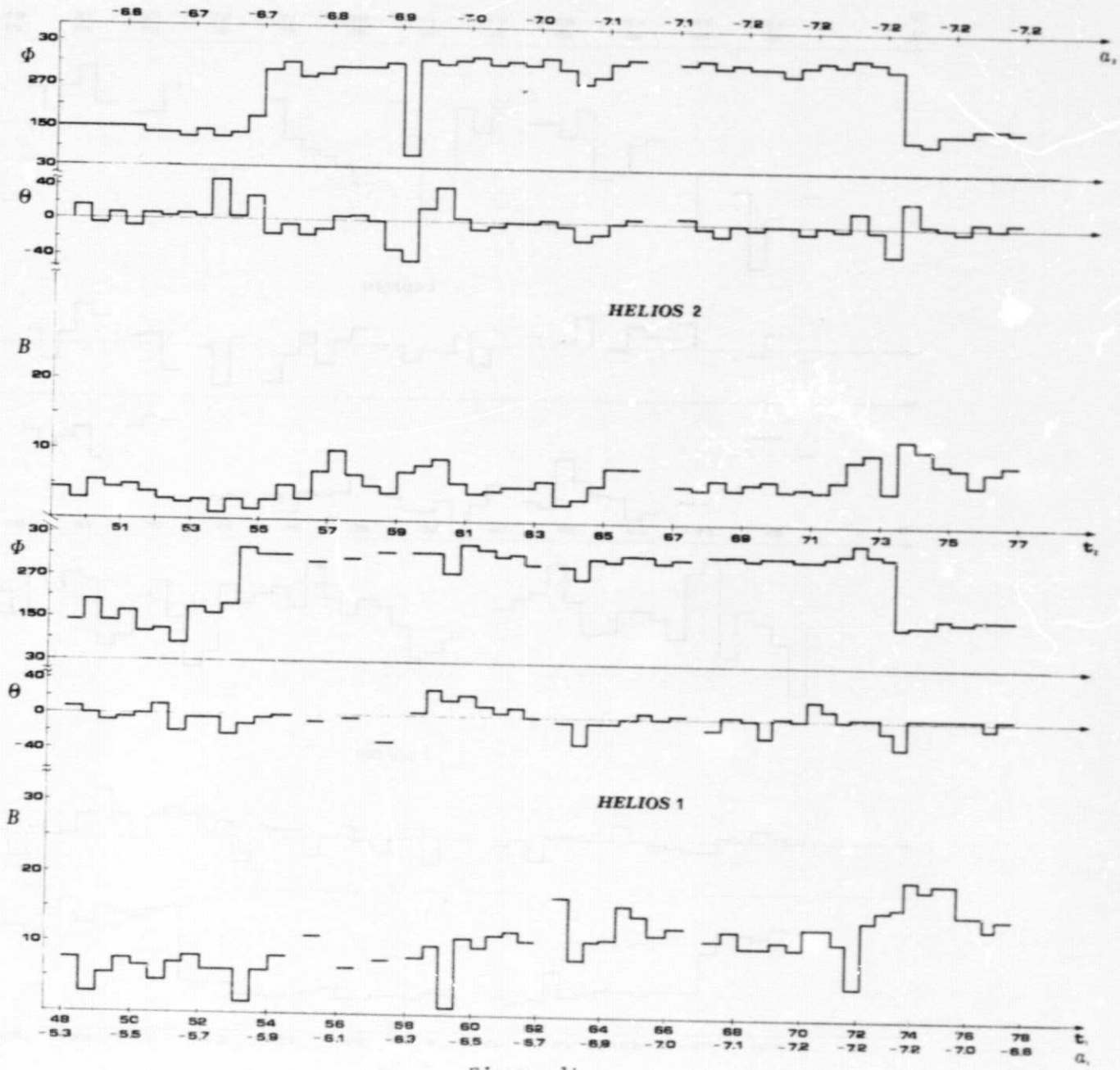

Figure 1b

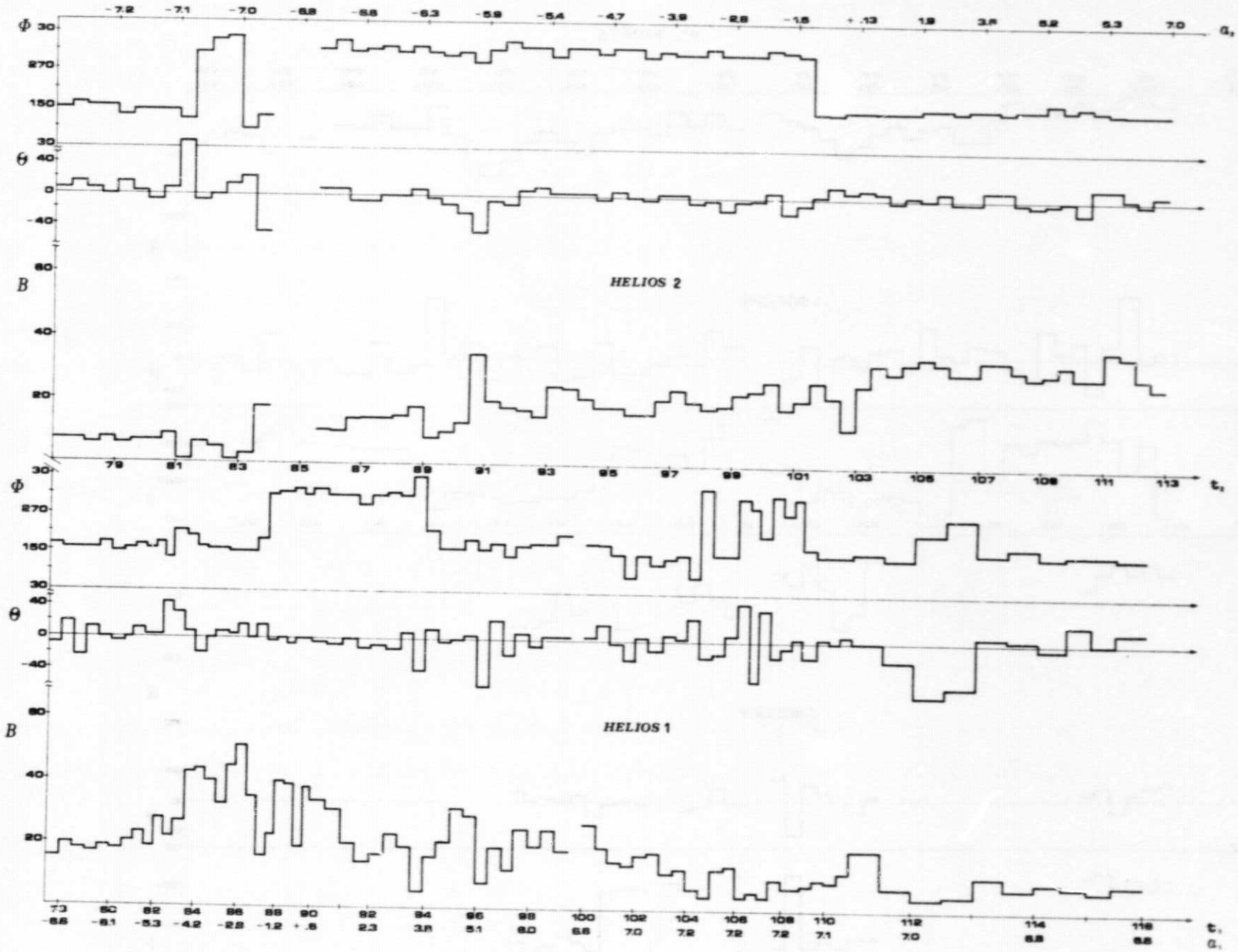

Figure 1c

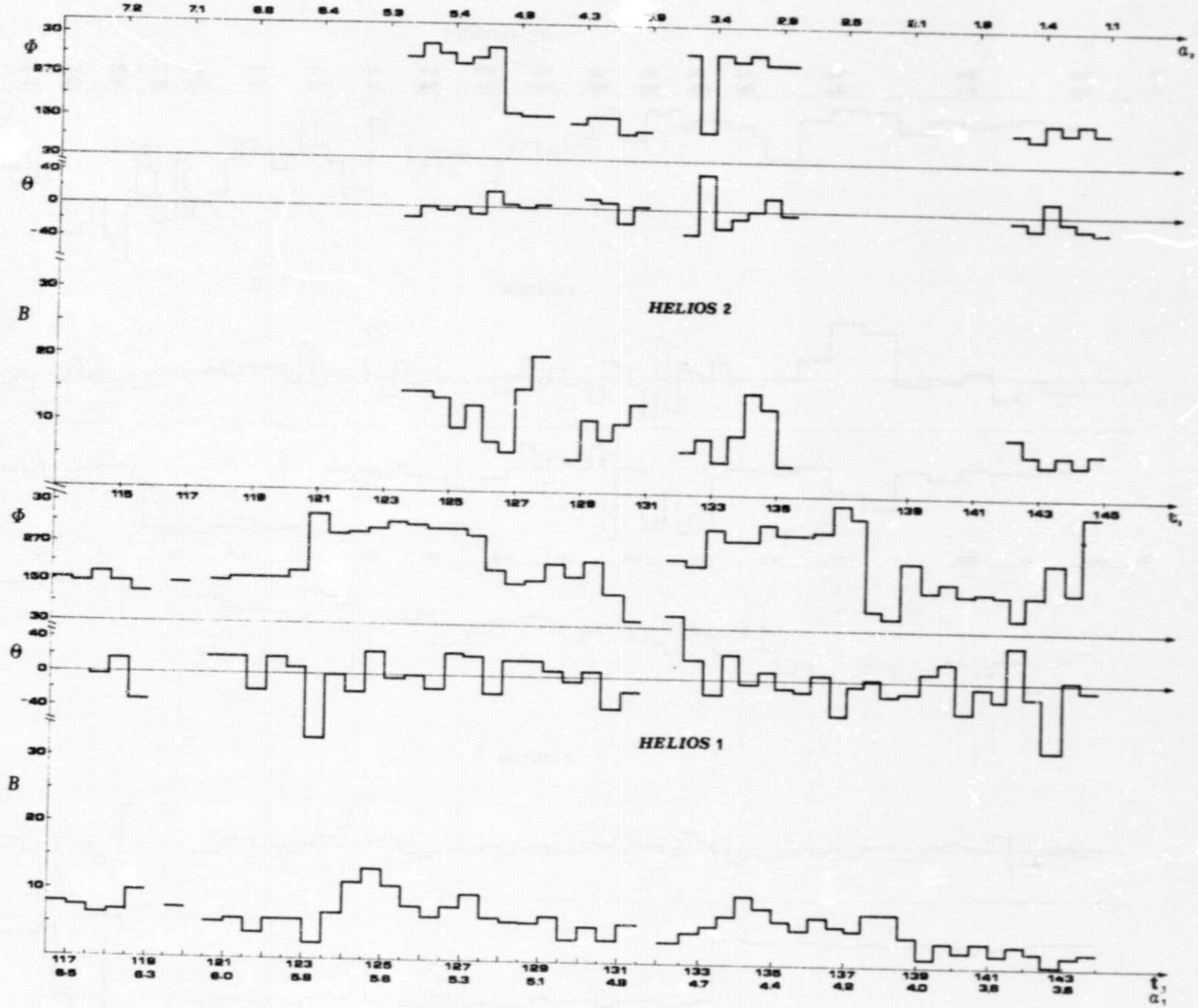

Figure 1d

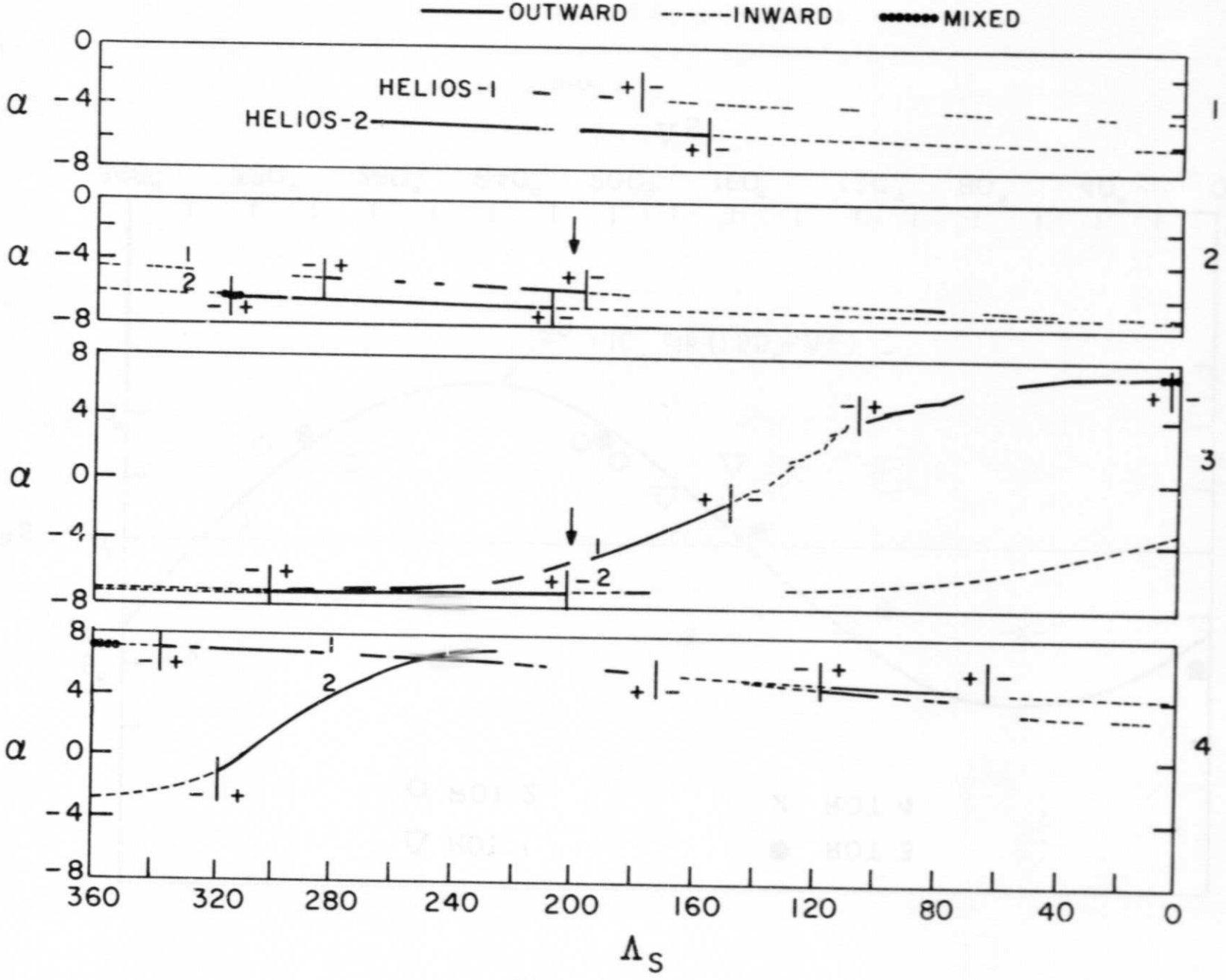
OUTWARD
INWARD
MIXED
HELIOS-1
HELIOS-2
α
0
-4
-8
8
4
1
2
3
4
360
320
280
240
200
160
120
80
40
0
Λs

Figure 2

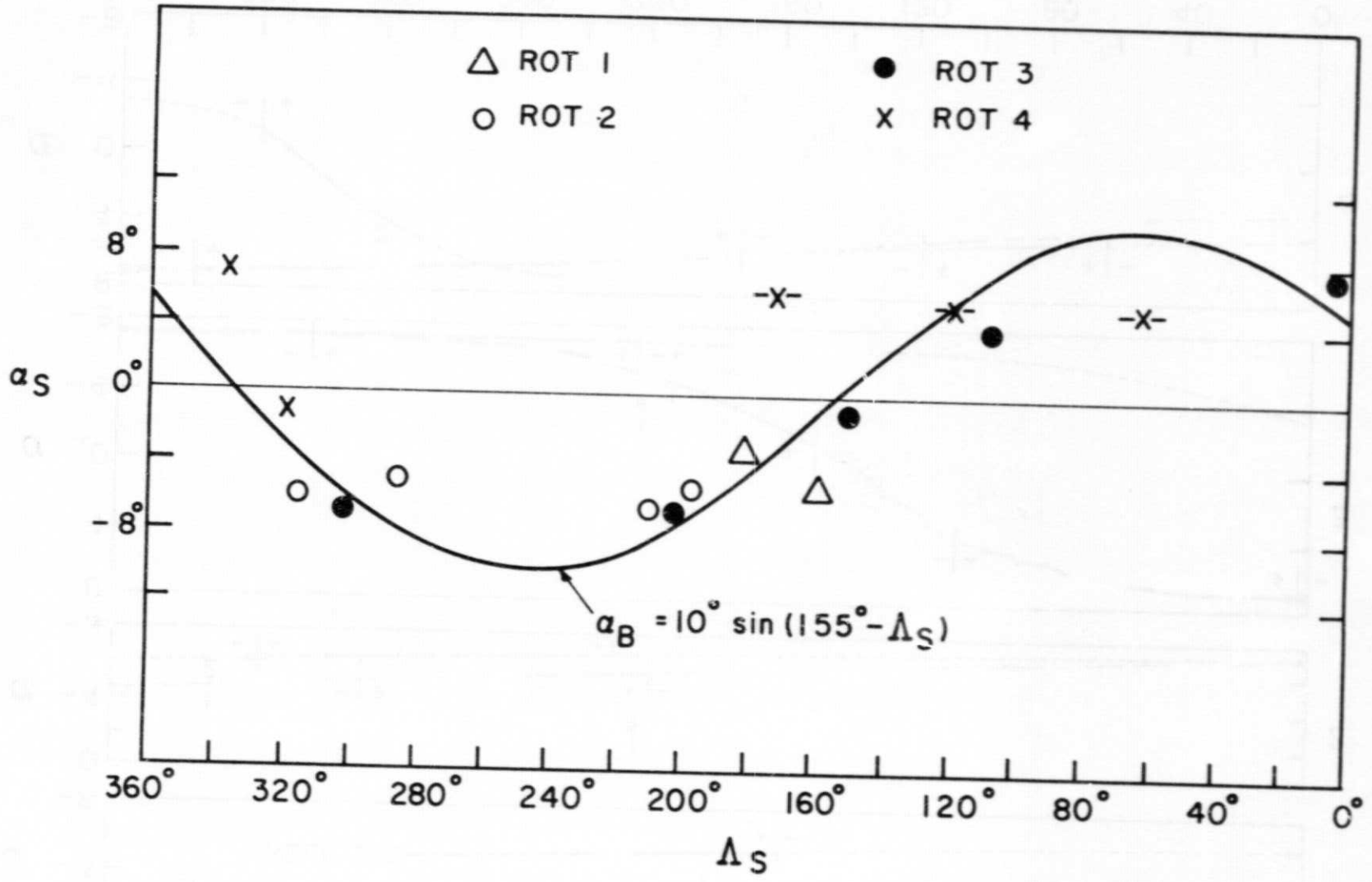
△ ROT 1
● ROT 3
○ ROT 2
X ROT 4
8°
0°
-8°
α_S
$\alpha_B = 10° \sin(155° - \Lambda_S)$
360°
320°
280°
240°
200°
160°
120°
80°
40°
0°
Λ_S

Figure 3

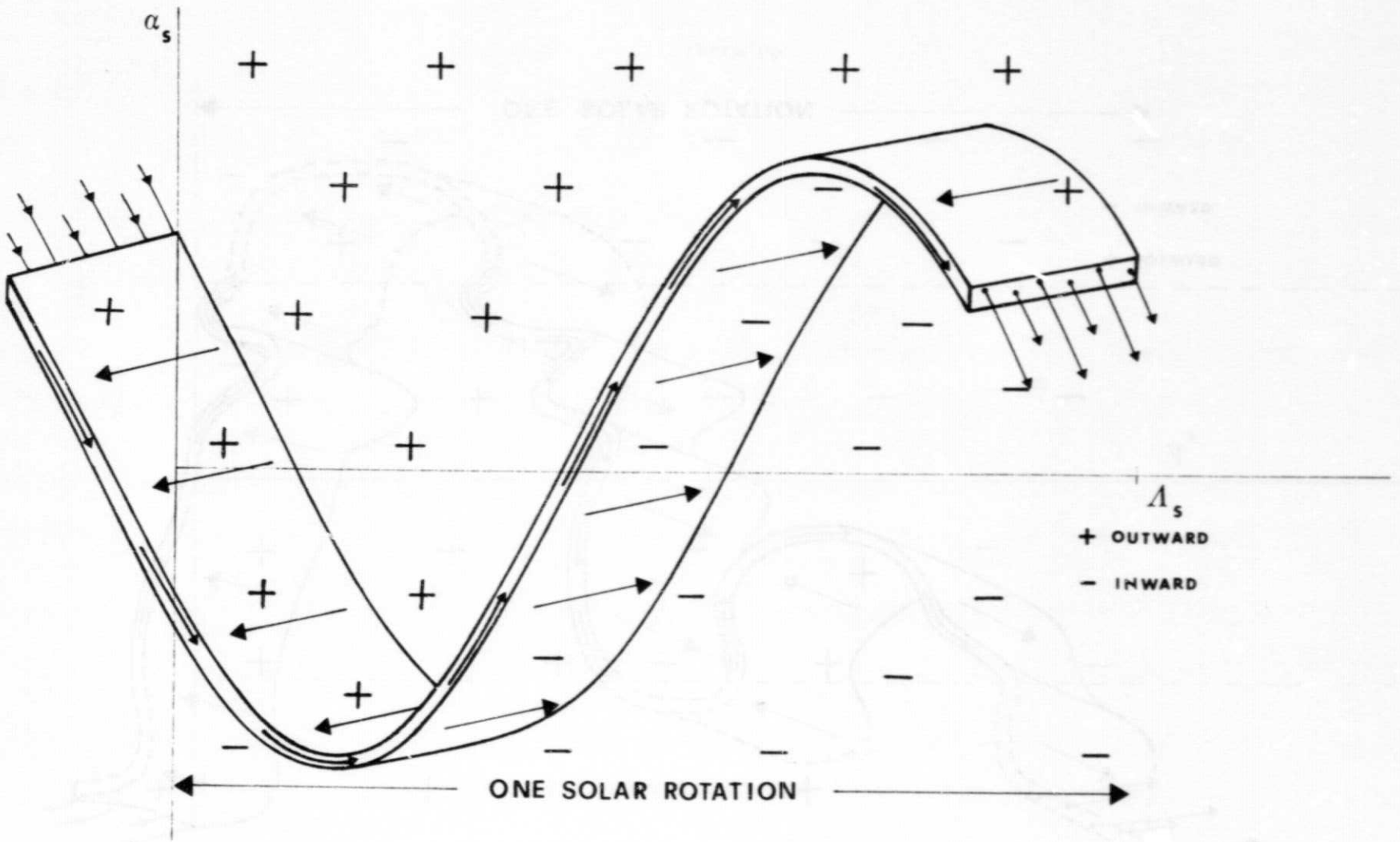

Figure 4a

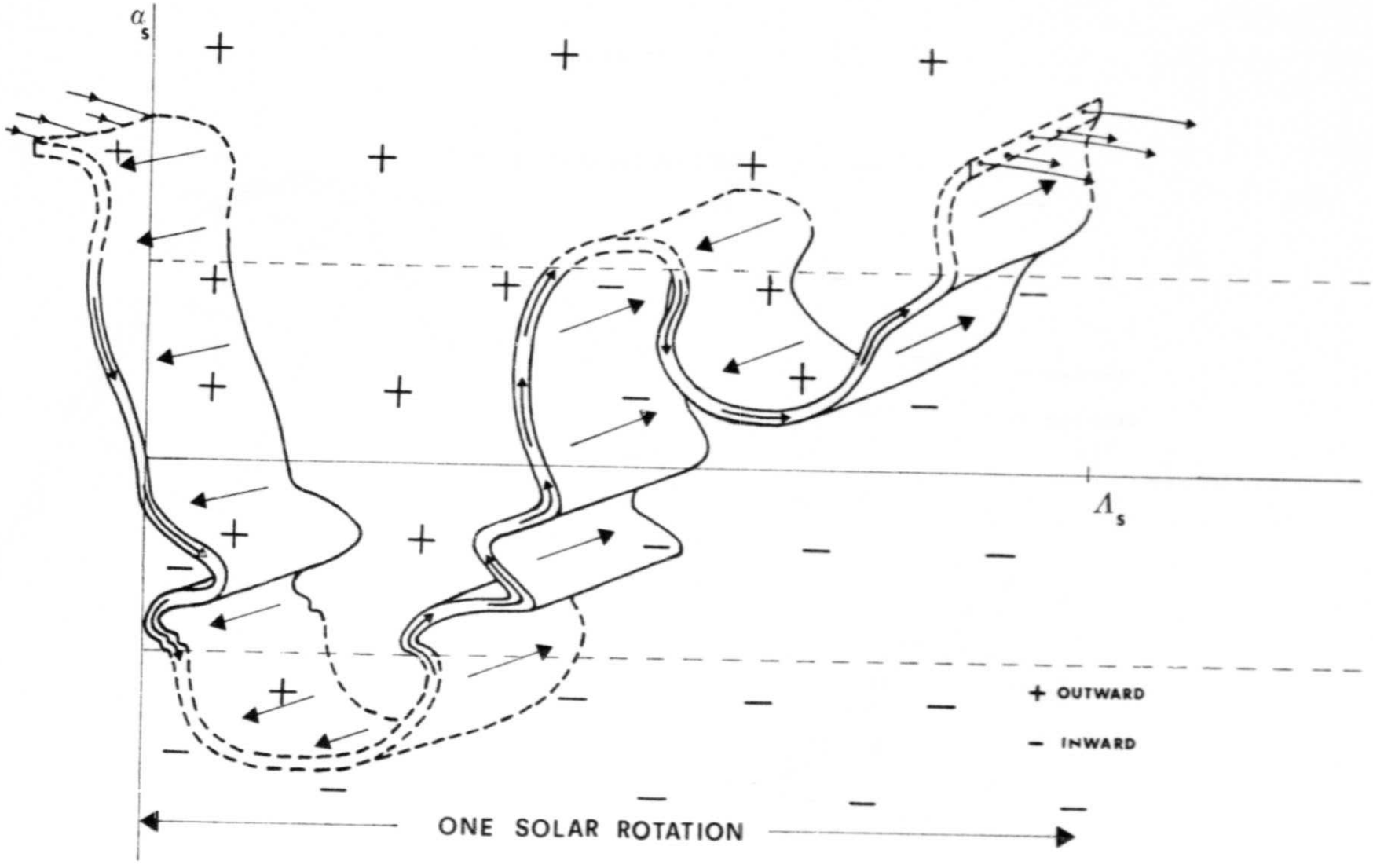

Figure 4b